



OPEN

## A novel fungal metal-dependent $\alpha$ -L-arabinofuranosidase of family 54 glycoside hydrolase shows expanded substrate specificity

Maria Lorenza Leal Motta<sup>1</sup>, Jaire Alves Ferreira Filho<sup>1</sup>, Ricardo Rodrigues de Melo<sup>2</sup>, Leticia Maria Zanphorlin<sup>2</sup>, Cleiton Aparecido dos Santos<sup>2</sup> & Anete Pereira de Souza<sup>1</sup>✉

*Trichoderma* genus fungi present great potential for the production of carbohydrate-active enzymes (CAZymes), including glycoside hydrolase (GH) family members. From a renewability perspective, CAZymes can be biotechnologically exploited to convert plant biomass into free sugars for the production of advanced biofuels and other high-value chemicals. GH54 is an attractive enzyme family for biotechnological applications because many GH54 enzymes are bifunctional. Thus, GH54 enzymes are interesting targets in the search for new enzymes for use in industrial processes such as plant biomass conversion. Herein, a novel metal-dependent GH54 arabinofuranosidase (ThABF) from the cellulolytic fungus *Trichoderma harzianum* was identified and biochemically characterized. Initial *in silico* searches were performed to identify the GH54 sequence. Next, the gene was cloned and heterologously overexpressed in *Escherichia coli*. The recombinant protein was purified, and the enzyme's biochemical and biophysical properties were assessed. GH54 members show wide functional diversity and specifically remove plant cell substitutions including arabinose and galactose in the presence of a metallic cofactor. Plant cell wall substitution has a major impact on lignocellulosic substrate conversion into high-value chemicals. These results expand the known functional diversity of the GH54 family, showing the potential of a novel arabinofuranosidase for plant biomass degradation.

Arabinofuranosidases (ABFs) (EC 3.2.1.55) are enzymes that are capable of cleaving residues of L-arabinofuranosyl present in various oligosaccharides and in polysaccharides such as hemicellulose; for this reason, they are interesting targets for biotechnological applications<sup>1</sup>. These enzymes are members of a group of glycoside hydrolases necessary for the degradation of polymeric substrates, such as arabinan, arabinoxytan and other polysaccharides that constitute the walls of plant cells<sup>2</sup>. ABFs are grouped into glycoside hydrolase (GH) families 3, 43, 51, 54 and 62, where GH54 including some enzymes described as bifunctional. However, there are few studies focusing on the functional specificity of this last family<sup>3</sup>.

Ravanel et al.<sup>4</sup> characterized an  $\alpha$ -L-arabinofuranosidase from *Penicillium purpurogenum* from the GH54 family, demonstrating that this family contains enzymes capable of acting synergistically with others and carrying out hydrolysis of different substrates in addition to arabinose and xylose. Thus, based on these characteristics presented by some enzymes in this group, further studies are needed to better understand their enzymatic mechanisms, especially with regard to their application for the conversion of complex substrates such as polysaccharides into bioproducts.

Vegetable biomass is a reservoir of sugars organized in complex regular structures represented by cellulose, hemicellulose and lignin<sup>5</sup>. Such structures need to be deconstructed for the release of sugar-free monomers, which can then be converted into high-added-value chemicals such as second-generation ethanol<sup>6</sup>. This process requires the enzymatic conversion of biomass, and hemicellulose is a biopolymer that requires a large complex of enzymes for its conversion due to its structural composition<sup>7</sup>.

<sup>1</sup>Dept. de Biologia Vegetal, Center for Molecular Biology and Genetic Engineering (CBMEG), University of Campinas (UNICAMP), Campinas, SP CEP 13083-875, Brazil. <sup>2</sup>Brazilian Biorenewables National Laboratory (LNBR), Brazilian Center for Research in Energy and Materials (CNPEM), Campinas, SP, 13083-100, Brazil. ✉email: anete@unicamp.br

For the enzymes to access the main chain of hemicellulose, it is necessary to remove side-chain substitutions, as they are one of the main reasons for the recalcitrance of plant biomass<sup>8,9</sup>. Thus, the search for enzymes that target hemicellulose substitutions is a promising approach for improving the saccharification of lignocellulosic material<sup>10</sup>. It is of interest to apply ABFs for this purpose because in addition, removing L-arabinose, some of these enzymes can act on other sugars involved in substitutions<sup>1</sup>.

These enzymes are particularly important in the genus *Trichoderma*, where they play a crucial physiological role<sup>11</sup>. This genus is composed of heterotrophic filamentous ascomycetous fungi that are capable of growing on different substrates and under different environmental conditions. There are several studies that have addressed the versatility of this genus, which range from applications in sugar and alcohol industries to the development of biofungicides<sup>12</sup>. *Trichoderma reesei* is of particular prominence within the group because of its recognized potential to produce several hydrolytic enzymes; however, other species of the genus, especially *Trichoderma harzianum*, have been shown to be as efficient as *T. reesei* in this regard<sup>13</sup>.

Therefore, in this study, we conducted the *in silico* bioprospecting of a new GH54 from *T. harzianum*. For this purpose, several approaches were used, such as RNA-seq, in addition to sequence analysis. The enzyme was also characterized biochemically with different substrates and metallic salts to determine their influence on the enzyme.

## Results

**Obtaining the sequence of ThABF and *in silico* characterization.** Through database searches, a sequence from *Trichoderma koningi* (AAA81024.1) was selected and used in the steps detailed in the methodology. With the resulting BLAST sequence, the *T. harzianum* CBS 226.95 genome was mapped. *T. harzianum* IOC-3844 RNA-seq reads and the target protein sequence (MT439956) were obtained. With this target protein sequence, a BLAST search was performed against the CAZy database, where our data suggest that ThABF is more similar to the GH54 family and that this family has several carbohydrate-binding models (CBMs; 1, 2, 6, 13 and 42), as shown in Supplementary Table S1.

Phylogenetic analysis of ThABF against sequences of the GH54 family (represented mainly by fungal and bacterial sequences) revealed great diversity between the sequences (Fig. 1a). The sequences used in the analysis are shown in Supplementary Table S2. The phylogenetic tree was divided into five groups that best explained this diversity: a Fungi group, containing only fungal enzymes, and Bacterium I to IV groups, containing bacterial enzymes. The predominant taxonomic groups were as follows: Fungi (all Ascomycetes), Bacteria I (Acidobacteria, Verrucomicrobia, Proteobacteria and Actinobacteria), Bacteria II (Actinobacteria and Proteobacteria), Bacteria III (Actinobacteria and Proteobacteria) and Bacteria IV (all Proteobacteria) (Supplementary Table S2).

The analysis of the domains of the sequences in the phylogenetic tree (Supplementary Table S2) showed that all members of Fungi contained ArabFuran-catal ( $\alpha$ -L-arabinofuranosidase B catalytic) and AbfB ( $\alpha$ -L-arabinofuranosidase B) domains, in addition to CBM 42 (Fig. 1b). In Bacterium I, the presence of CBMs 13 and 42 was observed, in addition to sequences with the following combinations of domains: ArabFuran-catal and AbfB; ArabFuran-catal, RICIN (ricin B lectin domain), LTD (lamin tail domain), NPCBM\_assoc (NEW3 domain of  $\alpha$ -galactosidase) and RPT1; and ArabFuran-catal and RICIN. All Bacterium II sequences exhibited only CBM 42 and ArabFuran-catal and AbfB domains.

The Bacterium III group sequences only CBM 13 and the following combinations of domains: ArabFuran-catal and two RPT1 domains; ArabFuran-catal and RICIN; and ArabFuran-catal and two RICIN domains. Bacterium IV was the smallest group; its sequences included no CBMs and were the most distinct from those of the other groups. The Bacterium IV members included only the ArabFuran-catal domain.

To analyze the similarity of the ThABF sequence with some arabinofuranosidases characterized as GH54 members in *Trichoderma*, alignment was performed (Fig. 2a). It was found that the target sequence was most similar to a sequence from *T. virens*, with a percent identity of 92.38%, followed by sequences from *T. reesei* (88.38%) and *T. koningi* (87.78%). The structure of the ThABF protein was also predicted, and the model that was used was an *Aspergillus kawachii*  $\alpha$ -L-arabinofuranosidase B with a C-score of 0.95, a TM-score of  $0.84 \pm 0.08$  and an RMSD of  $5.3 \pm 3.4$  Å (Fig. 2b).

**Production of recombinant protein and evaluation of the folding components.** With the sequence obtained from ThABF *in silico*, cloning and expression were performed. The enzyme was present in the insoluble fraction (Fig. 3a), and it was necessary to use the refolding approach described in the methodology, through which a protein of 53.44 kDa was purified (Fig. 3b). The recombinant ThABF sequence was used to evaluate the secondary and tertiary folding components of the enzyme since it was obtained through refolding. On the basis of the obtained circular dichroism profile, we identified rich  $\alpha$  helices in the ThABF structure (Fig. 3c). In the size exclusion chromatography (SEC), the protein was eluted in a single peak, presenting the characteristics of a monomer in solution (Fig. 3d). Thus, these analyses demonstrated that it was possible to obtain a protein with folding components through the refolding method used.

**Determination of enzyme specificity and tests with metal ions.** In the first experiment, enzyme activity was tested with the pNPara substrate because *in silico* analysis indicated that ThABF would present a relatively high affinity with this substrate. However, the detected activity was not significant, leading to the hypothesis that a cofactor is needed to activate the catalytic site of the enzyme. Thus, we evaluated the effects of different metals on the activity of ThABF (Fig. 4). It was observed that the enzyme requires a metal ion cofactor to exert its catalytic activity, since the control exhibited a profile similar to that of EDTA.  $\text{CuCl}_2$  had no effect on the enzyme's activity.  $\text{MgCl}_2$  had the greatest effect on the enzyme's activity among the eleven tested metal salts, followed by  $\text{MnCl}_2$ ,  $\text{CoCl}_2$ ,  $\text{CaCl}_2$  and  $\text{NiCl}_2$ . Despite the demonstration that ThABF requires a cofactor, its

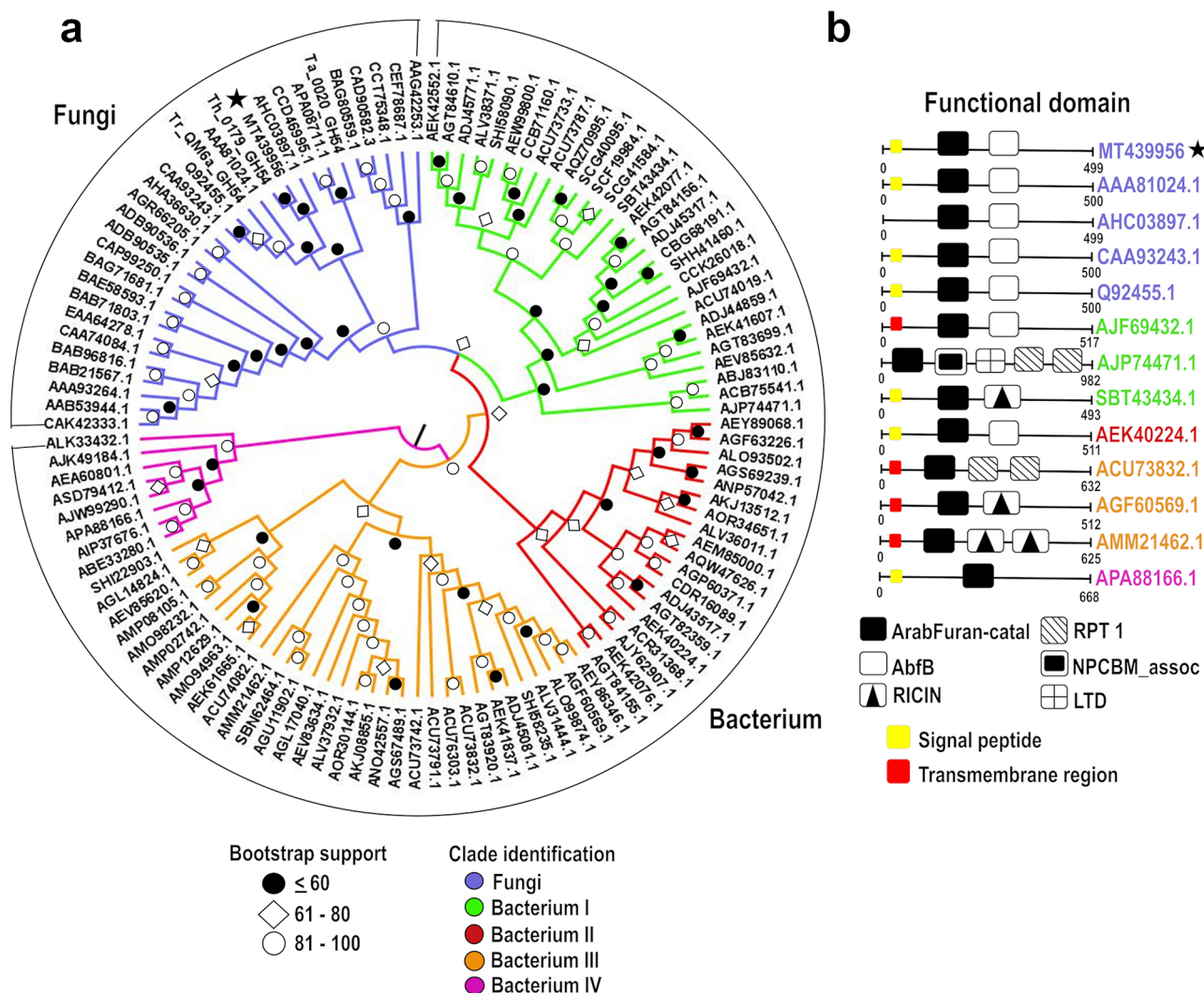


**Figure 1.** Phylogenetic analysis and sequence domains of the GH54 family. (a) Phylogenetic tree of the sequences. The star indicates the studied protein. Below the tree is a legend with the bootstrap values divided into  $\leq 60\%$ , 61–80 and 81–100. (b) Differences in the composition of domains in the sequences distributed in the groups. The identification of the groups is the same for A and B.

activity against pNPAra was not significantly increased; thus, a panel of chromogenic substrates derived from nitrophenol was tested to obtain information on ThABF enzymatic specificity (Table 1). The enzyme exhibited the greatest activity against pNPG, followed by pNPAp, pNPF and finally pNPAra.

**Optimization of pH and temperature conditions and enzymatic kinetics.** Following the selection of ThABF-specific substrates and ions, the optimization of pH and temperature was performed under different conditions to identify the ideal performance of the enzyme. As shown in Fig. 5a,b, maximum ThABF activity was observed at 55 °C and pH 6.5. The enzyme exhibited greater than 50% activity between temperatures of 45 and 60 °C. However, at lower temperatures, in the range of 20 to 40 °C, its activity was below 40%. ThABF exhibited a wide range of performance levels at pH values from 6.0 to 9.0, and the optimal pH was shown to be 6.5 in sodium phosphate buffer. At pH 4 to 5.5, enzyme activity decreased significantly. Experiments were carried out to examine the kinetics of ThABF with the substrates selected in the specificity tests; the parameters  $V_{max}$ ,  $K_m$ , and  $K_{cat}/K_m$  were calculated, and the results are shown in Table 2. The curves constructed with the substrates pNPG and pNPAra are shown in Fig. 5c,d.

## Discussion

Arabinofuranosidases are enzymes that, in addition to acting on L-arabinose, can also degrade other types of sugars and can be applied in various industrial processes<sup>1,14</sup>. In this work, we bioprospected an arabinofuranosidase from the metal-dependent GH54 family from *T. harzianum* and demonstrated that it showed expanded activity against other substrates. This enzyme can be introduced in enzymatic cocktails to assist in the hydrolysis of hemicellulose, since this biopolymer is present in approximately 50% of the most diverse sources of plant biomass, and its degradation requires highly diverse enzymes due to its structural complexity<sup>15–18</sup>.





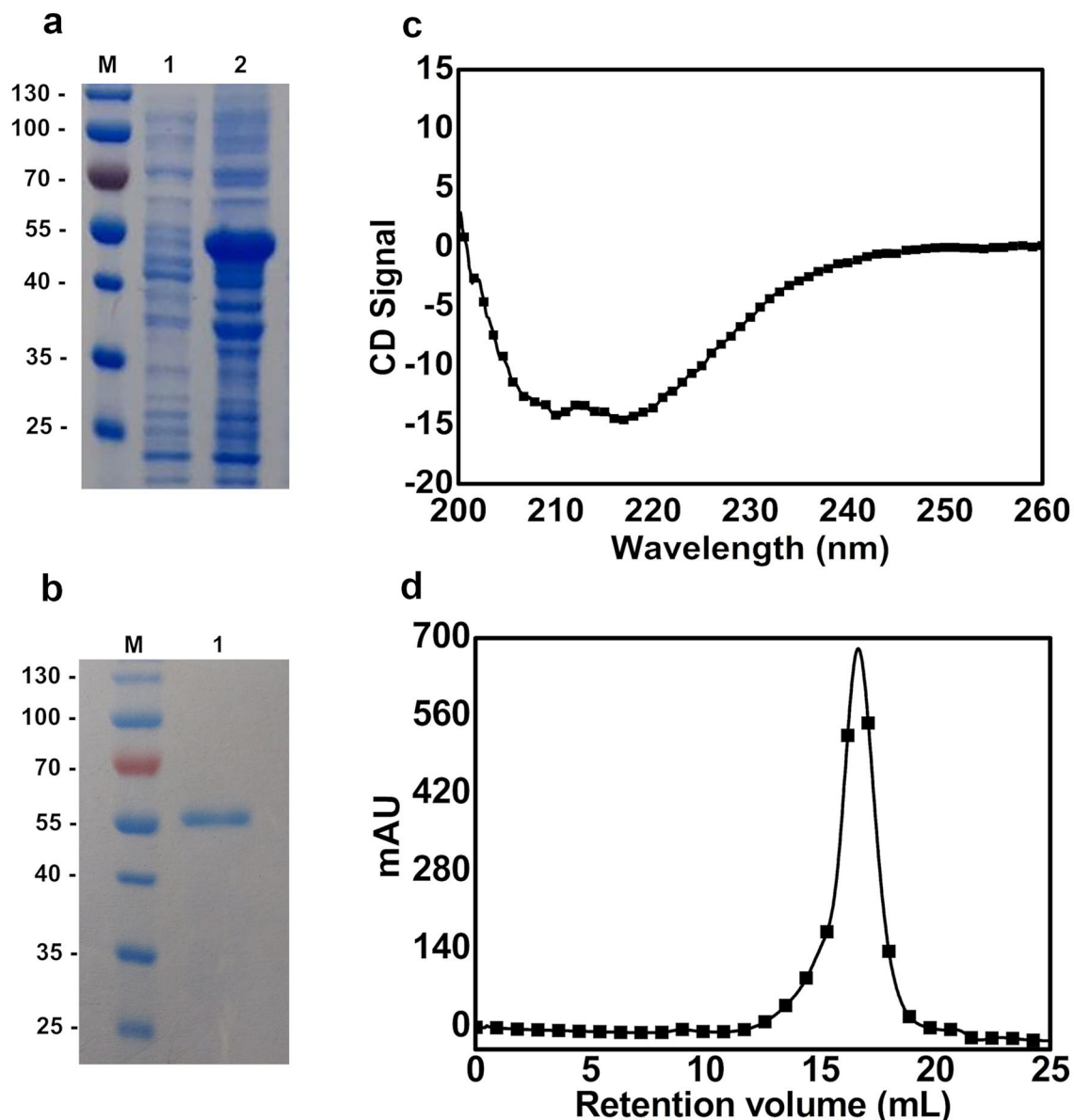


**Figure 3.** SDS-PAGE in 12% gels showing purification results and graphs of secondary and tertiary folding analyses. **(a)** Gel containing the soluble (1) and insoluble (2) fractions; M indicates the marker. **(b)** Gel containing purified ThABF, with a size of approximately 53.44 kDa (1), and a marker (M). Both gels **(a)** and **(b)** were stained for 30 min in a dye solution with Coomassie blue. The whole gels from the ThABF purification and from the soluble and insoluble fractions are shown in Supplementary Figs. S1 and S2. **(c)** Analysis of secondary folding components of the recombinant enzyme by circular dichroism. **(d)** Analytical size exclusion chromatography of ThABF.

activity may be related to some modification of the active site of these enzymes, and resolution of their structures would provide a better understanding of this enzymatic activity toward different substrates, as only one structure in the family has been resolved to date<sup>24</sup>. At the time of writing the present report, 19 enzymes had been characterized in this family, among which only 6 have been tested on different types of synthetic substrates<sup>4,19,30,31</sup>. In addition, as demonstrated via *in silico* analyses, there are several unstudied proteins of this family harboring domains related to the hydrolysis of galactose, among other types of sugars. This demonstrates the limitation of studies involving enzymes of this family of GHs.

The data obtained in the tests with metallic cofactors showed that the enzyme was dependent on metals. This role of  $Mg^{2+}$  has been reported for other enzymes; there are several hypotheses regarding how magnesium acts on these enzymes, one of which is that it helps maintain the conformation of the active site<sup>32</sup>. The analysis of the optimal conditions of the enzyme showed that ThABF presents characteristics similar to those of other fungal arabinofuranosidases of the GH54 family, making it quite adaptable to changes in the conditions imposed in several types of biotechnological processes, such as the hydrolysis of plant biomass<sup>1</sup>.

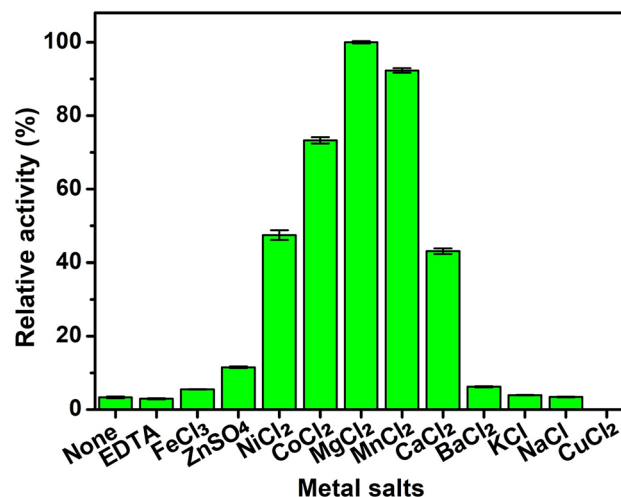


**Figure 4.** Relative activity of ThABF in the presence of different metallic ions.

Synthetic substrates	Relative activity (%)
$\beta$ -D-Galactopyranoside	100 $\pm$ 0
$\alpha$ -D-Arabinopyranoside	61.72 $\pm$ 0
$\beta$ -D-Fucopyranoside	21.79 $\pm$ 0.15
$\alpha$ -D-Arabinofuranoside	4.97 $\pm$ 0.13
$\alpha$ -D-Glucopyranoside	1.12 $\pm$ 0.03
$\alpha$ -L-Fucopyranoside	0.69 $\pm$ 0.60
$\alpha$ -L-Ramnopiranoside	0.44 $\pm$ 0.53
$\beta$ -D-Glucopyranoside	0.34 $\pm$ 0.09
$\alpha$ -D-Xylopyranoside	0.26 $\pm$ 0.05
$\alpha$ -D-Mannopyranoside	0.25 $\pm$ 0.05
$\alpha$ -D-Galactopyranoside	0.16 $\pm$ 0.09
$\beta$ -D-Cellobioside	0.09 $\pm$ 0.04
$\beta$ -D-Xylopyranoside	0.07 $\pm$ 0.09
$\beta$ -D-Mannopyranoside	0 $\pm$ 0.05

**Table 1.** Relative activity of ThABF against different synthetic substrates.

Based on the results presented above, ThABF has the potential to be used in the saccharification of lignocellulosic material, mainly because it acts on different types of sugars that constitute the side chains of hemicellulose<sup>33,34</sup>. These side chains contribute to the recalcitrancy of plant biomass due to its diverse structural composition<sup>2,35</sup>. The removal of hemicellulose makes it less recalcitrant, improving the hydrolysis process<sup>8,9</sup>. For this purpose, enzymes such as arabinofuranosidases that act on these sugars are necessary<sup>34</sup>.

In conclusion, the present study reports the *in silico* bioprospection, expression, purification and biochemical characterization of a GH54-dependent metal with expanded substrate specificity that acts in a wide pH range. These characteristics indicate the potential to use this enzyme in industrial bioprocesses, such as the saccharification of plant biomass. For future studies, it would be interesting to test the enzyme on different types of complex substrates, in addition to solving its structure to investigate the structural basis of the substrate specificity of ThABF.

## Methods

**In silico data mining, RNA-Seq read mapping and phylogenetic analyses of ThABF.** A search for sequences of bifunctional *Trichoderma* enzymes that act on hemicellulose was carried out in the NCBI non-redundant protein<sup>36</sup>, UniProt and CAZy databases. With the selected sequence, a BLASTP search was performed versus the genome of *T. harzianum* CBS 226.95 (TaxID: 983964) in the NCBI database. The most similar sequence was used to map the RNA-Seq reads of the *T. harzianum* IOC-3844 data generated in the work of Horta et al.<sup>37</sup> and, thus, obtain the sequence of the specific protein of the target lineage. For mapping, CLC *Genomics Workbench software* (CLC bio—v4.0; Finlandsgade, Dk) was used. Analyses of physical-chemical parameters were also performed with ProtParam; the presence of signal peptides was evaluated on the SignalP-5.0 server; domain prediction was conducted with SMART; and protein structure prediction was conducted with I-TASSER.

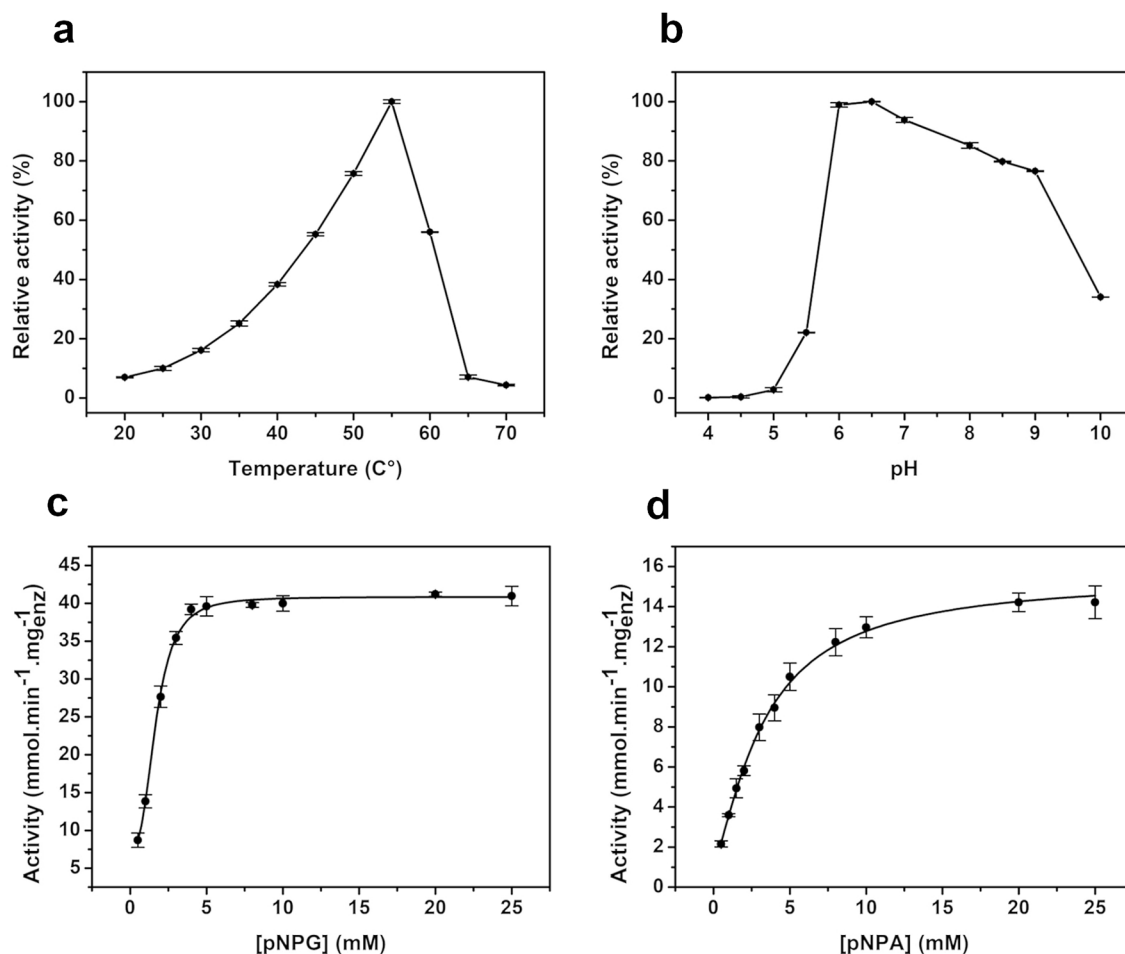


**Figure 5.** Biochemical characterization of ThABF. Relative activity of the recombinant protein at temperatures of 20 to 70 °C (a) and in the pH range of 4 to 10 (b). Enzymatic kinetics of TiBgal54A with the substrates pNPG (c) and pNPA (d).

	Vmax (mmol min <sup>-1</sup> mg <sup>-1</sup> enz)	km (mM)	Kcat (s <sup>-1</sup> )	Kcat/km (M <sup>-1</sup> s <sup>-1</sup> )
pNPG	40.85 ± 0.27	1.68 ± 0.12	35.53	2.11 × 10 <sup>4</sup>
pNPAP	15.47 ± 0.37	3.30 ± 0.16	13.45	4.07 × 10 <sup>3</sup>
pNPF	41.03 ± 4.02	6.51 ± 1.00	35.68	5.48 × 10 <sup>3</sup>
pNPAPra	1.85 ± 0.43	6.75 ± 3.24	1.61	2.38 × 10 <sup>2</sup>

**Table 2.** Kinetic parameters of ThABF against selected substrates.

A BLASTP search of the sequence resulting from mapping was performed versus the CAZy database, and different enzymes of the GH54 family were then selected to perform phylogenetic analysis. The sequences were aligned using *ClustalW*<sup>38</sup> implemented in *Molecular Evolutionary Genetics Analysis software*, version 7.0<sup>39</sup>. Gaps were removed manually, and incomplete or difficult-to-align sequences were excluded from the analysis. Phylogenetic analyses were performed with *MEGA7* using *maximum likelihood* (ML)<sup>40</sup> inference based on the Jones–Taylor–Thornton (JTT) model with 1000 *bootstrap*<sup>41</sup> repetitions for each analysis. The tree, drawn to scale, was obtained automatically by applying the *neighbor-joining* BioNJ algorithms to a matrix of distances in pairs estimated using the JTT model and the topology with the highest log probability values. The trees were visualized and edited using the program *Figtree*<sup>42</sup>.

**Heterologous production and refolding of ThABF.** The ThABF gene was cloned into the pET-28a (+) vector using the standard gene cloning protocol of Sambrook<sup>43</sup> with the aid of the forward primer TAAGAATTC GGGCCCTGTGA and the reverse primer TGGTCGACTTAAGCAAAGCTGG. The recombinant plasmids were transformed into *Escherichia coli* Rosetta (Novagen, Darmstadt, Germany) for protein overexpression.

Transformed *E. coli* Rosetta cells were grown to an optical density of approximately 0.8 at 800 nm. To trigger the transcription of the ThABF gene, it was inserted in a culture containing IPTG at 0.4 mM. Then, the cells



were incubated overnight at 25 °C, harvested by centrifugation and resuspended in 50 mL of buffer A (250 mM NaCl, 40 mM sodium phosphate, 20 mM imidazole, 3 mM MgCl<sub>2</sub>, 1 mM EDTA and pH 8.0), 1 mg/mL lysozyme and 1 mM PMSF (phenylmethylsulfonyl fluoride) for 30 min with shaking on ice. The cells were disrupted by sonication, and the soluble fraction was obtained by centrifugation (16,000 rpm, 40 min, 4 °C).

After rupturing the cells and resuspending the inclusion bodies, the refolding protocol of Santos et al.<sup>28</sup> was applied. The pellet was resuspended in 15 mL of buffer A containing 1 M urea. Then, sonication and centrifugation (16,000 rpm, 15 min, 4 °C) were performed 6 times. Dialysis was subsequently performed under agitation *overnight* with buffer A plus 0.4 M arginine, followed by centrifugation (10,000 rpm, 10 min, 4 °C). The concentrations of the purified proteins were determined spectroscopically using the molar extinction coefficient ( $\epsilon$ ) predicted on the basis of the amino acid sequence, and sample purity was estimated by polyacrylamide gel electrophoresis with 12% sodium dodecyl sulfate (SDS-PAGE).

**Analysis of folding components.** The far-UV CD spectra of ThABF were collected using a Jasco model J-810 spectropolarimeter from the National Biorenewables Laboratory (LNBR) coupled to a Peltier control system (PFD 425S-Jasco). The CD spectra were generated using the purified recombinant protein at a concentration of approximately 1.024 mg/mL in 10 mM sodium phosphate buffer, pH 8.0. A total of 12 accumulations were recorded within the range of 260 to 208 nm at a rate of 50 nm min<sup>-1</sup> using a quartz cuvette with a travel length of 1 mm, and the results were averaged.

The tertiary folding components of the recombinant refolded ThABF were evaluated by analytical SEC using a Superdex 200 10/300 GL column (GE Healthcare, Uppsala, Sweden). The protein sample at a concentration of approximately 0.56 mg/mL was dialyzed against buffer A, and gel filtration was then performed at a flow rate of 0.5 mL min<sup>-1</sup>. The elution fractions from each chromatographic run were collected and analyzed by 12% SDS-PAGE.

**Biochemical characterization.** The substrate specificity of ThABF was tested with the following pNP glycosides:  $\alpha$ -D-arabinopyranoside (pNPAP),  $\beta$ -D-galactopyranoside (pNPG),  $\alpha$ -D-arabinofuranoside (pNPFA),  $\beta$ -D-fucopyranoside (pNPF),  $\alpha$ -D-glucopyranoside,  $\alpha$ -D-xylopyranoside,  $\alpha$ -D-mannopyranoside,  $\alpha$ -L-rhamnopyranoside,  $\alpha$ -L-fucopyranoside,  $\beta$ -D-glucopyranoside,  $\alpha$ -D-galactopyranoside,  $\beta$ -D-xylopyranoside,  $\beta$ -D-cellobioside and  $\beta$ -D-mannopyranoside. A 10 mM concentration of pNPs was used in the tests, which were conducted in 100 mM sodium phosphate buffer, pH 6.5, at 55 °C for 10 min. The reactions were stopped with 100 mM CaCO<sub>3</sub>, and the released pNP was quantified spectrophotometrically at 410 nm.

After selecting the substrates against which ThABF exhibited activity, its activity was tested with different 1 mM concentrations of different metal salts (CaCl<sub>2</sub>, KCl, NaCl, MgCl<sub>2</sub>, MnCl<sub>2</sub>, CoCl<sub>2</sub>, ZnSO<sub>4</sub>, CuCl<sub>2</sub>, NiCl<sub>2</sub>, FeCl<sub>3</sub> and BaCl<sub>2</sub>) and EDTA. Before these tests, any metal ions that could interfere with the analysis were removed via two dialysis steps performed on the recombinant protein overnight under agitation. First, 15 mM EDTA was added to chelate the metals present in the sample, and the protein was then transferred to a buffer containing 10 mM sodium phosphate. Subsequently, the tested chemicals were individually incubated with the recombinant enzyme; the reactions occurred at 55 °C at pH 6.5 for 10 min with pNPG as the substrate.

After the selection of the ion with the greatest effect on the enzyme, it was used to optimize pH and temperature conditions. The optimal pH was determined by incubating 0.12 mg/mL of purified ThABF with 10 mM pNPG in buffers with pH levels ranging from 3.0 to 10.0 [sodium acetate buffer (100 mM, pH 3.0 to 5.0), sodium phosphate buffer (100 mM, pH 6.0 to 8.0) and Tris-NaCl (100 mM, pH 7.0 to 9.0)]. The mixtures were incubated at 55 °C for 10 min, and the released pNP was quantified spectrophotometrically at 410 nm. The same conditions were applied to investigate the ideal temperature; these tests were conducted with Na<sub>2</sub>HPO<sub>4</sub> phosphate buffer (pH 6.5, 100 mM) at a temperature range of 20 to 70 °C. Subsequently, the pH test was repeated at the identified temperature.

After performing the above tests, assays of enzymatic kinetics were performed at pH 6.5 at 55 °C for 10 min, with pNPG, pNPAP, pNPF and pNPFA as substrates. The parameters Km, Vmax, and Kcat and the Kcat/Km ratio were obtained by plotting using the Lineweaver–Burk method, where the plots were constructed by plotting the substrate concentration on the x axis and the speed of the enzymatic reaction on the y axis using the OriginPro 8.5.0 program. The experiments were performed in triplicate at an ideal temperature and pH. A unit of enzymatic activity was defined as the amount of enzyme required to release 1  $\mu$ mol of p-nitrophenol per minute under the tested conditions.

### Accession codes

The protein sequence in this study has been deposited at the National Center for Biotechnology Information (NCBI) under accession code MT439956.

Received: 18 December 2020; Accepted: 10 May 2021

Published online: 26 May 2021

### References

1. Poria, V., Saini, J. K., Singh, S., Nain, L. & Kuhad, R. C. Arabinofuranosidases: characteristics, microbial production, and potential in waste valorization and industrial applications. *Bioresour. Technol.* **304**, 123019 (2020).
2. Basu, P. Biomass characteristics. In *Biomass Gasification Design Handbook* (ed. Basu, P.) 27–63 (Elsevier Inc., 2010).
3. Lagaert, S., Pollet, A., Courtin, C. M. & Volckaert, G.  $\beta$ -Xylosidases and  $\alpha$ -L-arabinofuranosidases: accessory enzymes for arabinoxylan degradation. *Biotechnol. Adv.* **32**, 316–332 (2014).
4. Ravanal, M. C. & Eyzaguirre, J. Heterologous expression and characterization of  $\alpha$ -L-arabinofuranosidase 4 from *Penicillium purpurogenum* and comparison with the other isoenzymes produced by the fungus. *Fungal Biol.* **119**, 641–647 (2015).



5. Tursi, A. A review on biomass: importance, chemistry, classification, and conversion. *Biofuel Res. J.* **6**, 962–979 (2019).
6. Francocci, F. & Reça, I. B. Composition of plant biomass biotech engineering of cell wall to optimize biofuel production. In *Bio-transformation of Agricultural Waste and By-Products* (eds Francocci, F. & Reça, I. B.) 219–236 (Elsevier Inc., 2016).
7. Chen, H. Lignocellulose biorefinery conversion engineering. In *Lignocellulose Biorefinery Engineering* (ed. Chen, H.) 87–124 (Elsevier, 2015).
8. Zoghalmi, A. & Paës, G. Lignocellulosic biomass: understanding recalcitrance and predicting hydrolysis. *Front. Chem.* **7**, 874 (2019).
9. Melati, R. B. *et al.* Key factors affecting the recalcitrance and conversion process of biomass. *Bioenergy Res.* **12**, 1–20 (2019).
10. Chandel, A. K. *et al.* Bioconversion of hemicellulose into ethanol and value-added products: commercialization, trends, and future opportunities. In *Advances in Sugarcane Biorefinery* (eds Chandel, A. K. *et al.*) 97–134 (Elsevier, 2018).
11. Adav, S. S. & Sze, S. K. *Trichoderma* secretome: an overview. In *Biotechnology and Biology of Trichoderma* (eds Adav, S. S. & Sze, S. K.) 103–114 (Elsevier, 2014).
12. Druzhinina, I. S. *et al.* Massive lateral transfer of genes encoding plant cell wall-degrading enzymes to the mycoparasitic fungus *Trichoderma* from its plant-associated hosts. *PLoS Genet.* **14**, 1–33 (2018).
13. Horta, M. A. C. *et al.* Transcriptome profile of *Trichoderma harzianum* IOC-3844 induced by sugarcane bagasse. *PLoS ONE* **9**, 1–17 (2014).
14. Dimarogona, M. & Topakas, E. Regulation and heterologous expression of lignocellulosic enzymes in *Aspergillus*. In *New and Future Developments in Microbial Biotechnology and Bioengineering: Aspergillus System Properties and Applications* (eds Dimarogona, M. & Topakas, E.) 171–190 (Elsevier B.V., 2016).
15. Yeo, J. Y., Chin, B. L. F., Tan, J. K. & Loh, Y. S. Comparative studies on the pyrolysis of cellulose, hemicellulose, and lignin based on combined kinetics. *J. Energy Inst.* **92**, 27–37 (2019).
16. Biely, P., Singh, S. & Puchart, V. Towards enzymatic breakdown of complex plant xylan structures: state of the art. *Biotechnol. Adv.* **34**, 1260–1274 (2016).
17. Fry, S. C. Cell walls and fibers. In *Encyclopedia of Applied Plant Sciences* (ed. Fry, S. C.) 75–87 (Elsevier, 2003).
18. Chen, D. *et al.* Investigation of biomass torrefaction based on three major components: hemicellulose, cellulose, and lignin. *Energy Convers. Manag.* **169**, 228–237 (2018).
19. Margolles-Clark, E., Tenkanen, M., Nakari-Setälä, T. & Penttilä, M. Cloning of genes encoding alpha-L-arabinofuranosidase and beta-xylosidase from *Trichoderma reesei* by expression in *Saccharomyces cerevisiae*. *Appl. Environ. Microbiol.* **62**, 3840–3846 (1996).
20. Hazes, B. The (QxW)<sub>3</sub> domain: a flexible lectin scaffold. *Protein Sci.* **5**, 1490–1501 (1996).
21. Spinette, S. *et al.* Ufd2, a novel autoantigen in scleroderma, regulates sister chromatid separation. *Cell Cycle* **3**, 1612–1618 (2004).
22. Hirabayashi, J., Dutta, S. K. & Kasai, K. I. Novel galactose-binding proteins in annelida. *J. Biol. Chem.* **273**, 14450–14460 (1998).
23. Naumoff, D. G. Phylogenetic analysis of -galactosidases of the GH27 family. *Mol. Biol.* **38**, 388–400 (2004).
24. Miyanaga, A. *et al.* The family 42 carbohydrate-binding module of family 54 alpha-L-arabinofuranosidase specifically binds the arabinofuranose side chain of hemicellulose. *Biochem. J.* **399**, 503–511 (2006).
25. Li, S. *et al.* Family 13 carbohydrate-binding module of alginate lyase from *Agarivorans* sp. L11 enhances its catalytic efficiency and thermostability, and alters its substrate preference and product distribution. *FEMS Microbiol. Lett.* **362**, 1–7 (2015).
26. Gielkens, M. *et al.* The abfB gene encoding the major alpha-L-arabinofuranosidase of *Aspergillus nidulans*: nucleotide sequence, regulation and construction of a disrupted strain. *Microbiology* **145**, 735–741 (1999).
27. Koseki, T. *et al.* Role of two alpha-L-arabinofuranosidases in arabinoxylan degradation and characteristics of the encoding genes from shochu koji molds, *Aspergillus kawachii* and *Aspergillus awamori*. *J. Biosci. Bioeng.* **96**, 232–241 (2003).
28. Santos, C. A. & Souza, A. P. Solubilization, folding, and purification of a recombinant peptidoglycan-associated lipoprotein (PAL) expressed in *Escherichia coli*. *Curr. Protoc. Protein Sci.* **92**, e53 (2018).
29. Santos, C. A. *et al.* Characterization of the TolB–Pal trans-envelope complex from *Xylella fastidiosa* reveals a dynamic and coordinated protein expression profile during the biofilm development process. *Biochim. Biophys. Acta Proteins Proteom.* **1854**, 1372–1381 (2015).
30. de Wet, B. J. M., Matthew, M. K. A., Storbeck, K. H., van Zyl, W. H. & Prior, B. A. Characterization of a family 54 alpha-L-arabinofuranosidase from *Aureobasidium pullulans*. *Appl. Microbiol. Biotechnol.* **77**, 975–983 (2008).
31. Wan, C. F., Chen, C. T., Li, Y. K. & Huang, L. Expression, purification and characterization of a bifunctional alpha-L-arabinofuranosidase/beta-D-xylosidase from *Trichoderma koningii* G-39. *J. Chin. Chem. Soc.* **54**, 109–116 (2007).
32. Höhn, S., Virtanen, S. & Boccacini, A. R. Protein adsorption on magnesium and its alloys: a review. *Appl. Surf. Sci.* **464**, 212–219 (2019).
33. Madeira, J. V. *et al.* Agro-industrial residues and microbial enzymes: an overview on the eco-friendly bioconversion into high value-added products. In *Biotechnology of Microbial Enzymes: Production, Biocatalysis and Industrial Applications* (eds Brahmachari, G. *et al.*) 475–511 (Elsevier Inc., 2017).
34. Liu, X. & Kokare, C. *Microbial Enzymes of Use in Industry. Biotechnology of Microbial Enzymes: Production, Biocatalysis and Industrial Applications* (Elsevier Inc., 2017).
35. Erbringerová, A., Hromádková, Z. & Heinze, T. Hemicellulose. In *Polysaccharides I* (ed. Heinze, T.) 1–67 (Springer, 2005).
36. Pearson, W. R. An introduction to sequence similarity (“homology”) searching. In *Current Protocol in Bioinformatics, Chapter 3, Unit 3.1.3.1.1-7* (2013).
37. Horta, M. A. C. *et al.* Network of proteins, enzymes and genes linked to biomass degradation shared by *Trichoderma* species. *Sci. Rep.* **8**, 1–11 (2018).
38. Thompson, J. D., Higgins, D. G. & Gibson, T. J. CLUSTAL W: improving the sensitivity of progressive multiple sequence alignment through sequence weighting, position-specific gap penalties and weight matrix choice. *Nucleic Acids Res.* **22**, 4673–4680 (1994).
39. Kumar, S., Stecher, G. & Tamura, K. MEGA7: molecular evolutionary genetics analysis version 7.0 for bigger datasets. *Mol. Biol. Evol.* **33**, 1870–1874 (2016).
40. Jones, D. T., Taylor, W. R. & Thornton, J. M. The rapid generation of mutation data matrices from protein sequences. *Comput. Appl. Biosci.* **8**, 275–282 (1992).
41. Felsenstein, J. Confidence limits on phylogenies: an approach using the bootstrap. *Soc. Study Evol.* **39**, 1–15 (1985).
42. Ferreira Filho, J. A., Horta, M. A. C., Beloti, L. L., Dos Santos, C. A. & de Souza, A. P. Carbohydrate-active enzymes in *Trichoderma harzianum*: a bioinformatic analysis bioprospecting for key enzymes for the biofuels industry. *BMC Genom.* **18**, 1–12 (2017).
43. Dong, L., Lv, L. B. & Lai, R. *Molecular Cloning. Dong wu xue yan jiu = Zoological research/“Dong wu xue yan jiu” bian ji wei yuan hui bian ji* (Yunnan Ren Min Chu Ban She, 2012).

## Acknowledgements

This work was supported by grants from the Fundação de Amparo à Pesquisa do Estado de São Paulo (FAPESP 2015/09202-0 and 2018/19660-4), Coordenação de Aperfeiçoamento de Pessoal de Nível Superior (CAPES) Computational Biology Program (CBP: Process number 88882.160095/2013-01) and Conselho Nacional de Desenvolvimento Científico e Tecnológico (CNPq: Process number 312777/2018-3; 430350/2018-0). MLLM received an MS fellowship from CAPES (CBP—88887.200427/2018-00); JAFF received a PhD fellowship from

CNPq (170565/2017-3) and a PD fellowship from CAPES (CBP—88887.334235/2019-00); RRM received a PD fellowship from FAPESP (17/14253-9); LMZ is a recipient of a research fellowship from FAPESP (19/08855-1); CAS received a PD fellowship from FAPESP (2016/19775-0) and an SWE PD fellowship from CAPES (CBP); and APS is the recipient of a research fellowship from CNPq (312777/2018-3). We thank the National Biorenewables Laboratory (LNBR).

### Author contributions

M.L.L.M. carried out all the experiments and wrote the manuscript. J.A.F.F. helped with the in silico analyses and wrote the manuscript. R.R.M. and L.M.Z. helped with the biochemical characterization. C.A.S. designed the experiments and wrote the manuscript. A.P.S. directed the general study and wrote the manuscript. All authors read and approved the manuscript.

### Competing interests

The authors declare no competing interests.

### Additional information

**Supplementary information** The online version contains supplementary material available at <https://doi.org/10.1038/s41598-021-90490-2>.

**Correspondence** and requests for materials should be addressed to A.P.S.

**Reprints and permissions information** is available at [www.nature.com/reprints](http://www.nature.com/reprints).

**Publisher's note** Springer Nature remains neutral with regard to jurisdictional claims in published maps and institutional affiliations.



**Open Access** This article is licensed under a Creative Commons Attribution 4.0 International License, which permits use, sharing, adaptation, distribution and reproduction in any medium or format, as long as you give appropriate credit to the original author(s) and the source, provide a link to the Creative Commons licence, and indicate if changes were made. The images or other third party material in this article are included in the article's Creative Commons licence, unless indicated otherwise in a credit line to the material. If material is not included in the article's Creative Commons licence and your intended use is not permitted by statutory regulation or exceeds the permitted use, you will need to obtain permission directly from the copyright holder. To view a copy of this licence, visit <http://creativecommons.org/licenses/by/4.0/>.

© The Author(s) 2021